Nigerian Research Journal of Chemical Sciences **(ISSN: 2682-6054)**
Vol. 7, Issue 2, 2019

PHOTOCATALYSIS OF Na/K-DOPED STRONTIUM FERRITE, $Sr_{1-x}M_xFeO_3$, BY CO-PRECIPITATION

Abdulwahab, I.

Department of Chemistry, Ahmadu Bello University, Zaria, Nigeria

Corresponding Email: *femiagie@gmail.com*

ABSTRACT

The precursors, $Fe(NO_3)_2.9H_2O$ and $Sr(NO_3)_2$, were used to prepare perovskite by coprecipitation method in distilled water using automated-shaking magnetic heater. Various amounts (x = 0.10 M and x = 0.20 M) of the dopants, Na and K, were added as $NaNO_3$ and KNO_3 precursors. Sodium dodecyl sulphate (SDS) was added to help in morphology control followed by the addition of NH_4OH as precipitating agent, filtered, oven-dried and annealed at temperature of 500 ^oC, 700 ^oC and 800 ^oC in muffle furnace. The Na/K-doped perovskites were characterized by Scanning electron microscopy (SEM) depicting hexagonal structure, with energy Dispersive X-ray Spectroscopy (EDS) quantitative and qualitative contents of the samples confirming the presence of the metals (Sr, Fe, Na, K,) in the wet chemical process. X-ray diffractometry (XRD) was performed and 0.267 nm crystallite size was obtained. The photocatalysis was carried out using methylene blue (MB) with K-doped sample, $Sr_{0.8}K_{0.2}FeO_3$, showing the highest photodegradation.

KEYWORDS: Coprecipitation, degradation, dopants, SDS.

INTRODUCTION

The Perovskite structure is $^{XII}A^{2+}\ ^{VI}B^{4+}\ X^{2-}{}_3$ with X^{2-} in the edge centres that could be oxygen or nitrogen. Natural compounds with this structure are Perovskite, Loparite and the Silicate Perovskitebridgmanite [1]. The earth's crust contains various types of Perovskite and the abundant ones are $MgSiO_3$ and $FeSiO_3$. The most common anionic part of Perovskite is oxygen leading to ABO_3, oxide Perovskite. However, halides and sulfide Perovskites are also obtainable [2]. Among the transition metal oxides, perovskite compounds of the type $R_{1-x}\ A_xBO_{3-\delta}$, where R is a rare earth metal, A is Ba, Ca, or Sr, Bis Fe, Mn, Co, or Ni, are of considerable importance, due to their interesting electrical, magnetic, and catalytic properties [3]. In particular, the Mn and

Fe compounds have been extensively studied as regards their magnetic and transport properties [4].

The metallic ferrite phases, $MFeO_3$, can exhibit different properties depending on the type M^+ used on the A-site. In particular $LaFeO_3$ is an antiferromagnetic insulator $SrFeO_3$ is metal and $CaFeO_3$ is a system with charge ordering $Fe^{iv} \longrightarrow Fe^{iv+x} + Fe^{iv-x}$ [5], where the spin and charge of perovskite depend on stoichiometry (the presence of oxygen vacancies in the lattice), temperature and external pressure. The band energy and atomic interractions of $SrFeO_3$perovskite were investigated in the framework of the density functional theory in the local spin density approximation using the tight-binding linear muffin-tin orbital method within the atomic sphere approximation and the augmented spherical wave method [6]. Strontium hexaferrite magnets are widely used in electrotechnical and radio industry, computer and medicinal techniques owing to a favorable combination of sufficiently high magnetic properties, chemical stability and low cost. It is well known that the coercive force of the hexaferrites depends mainly on the crystallite size; the high coercivity can be reached when the size of crystallites D is approximately 100 nm [7].

The basic structure of the organic-inorganic perovskites family is AMX_3. It consists of corner-sharing MX_4^{-6} octahedral, where X is typically an anion: O^{2-}, CI^- , Br^- or S^{2-}, and the M atom is generally a divalent metal that can adopt an octahedral anion coordination, such as Ge^{2+}, Sn^{2+}, Pb^{2+}, Co^{2+}, Fe^{2+}, Cu^{2+}, Ni^{2+}, Mn^{2+}, Cr^{2+}, Pd^{2+}, Cd^{2+}, Eu^{2+}, or Yb^{2+} [8]. Perovskitesnanomaterials have been known to possess numerous applications and uses industrially due to their interesting and fascinating multifunctional characteristics [9]. Perovskite sample will exhibit new properties when the particle size is reduced to the nanoscale [10]. Perovskite-type complex ferrites $La_{1-x}Sr_xFeO_3$ have attracted considerable attention because of their interesting electrical, magnetic and catalytic properties [11].

The band gap of BFO was expanded with the addition of Y and increased with the increase of the amount of Y. Whereas, the band gap decreased with the addition of rare earth transition metals such as La [12]. Zhang et al. [13] investigated the influence of La doping on the crystal structure and the photoabsorption tests revealed that doping with La had little influence on the optical property [14]. Deterioration under reducing atmosphere is sometimes important for the catalyst life of perovskites. Here, the variability of valence principally determines the reducibility, for

example, $LaMnO_3$ > $LaFeO_3$ > $LaCoO_3$. Most perovskites are basic and rather readily react with acidic gases resulting in deactivation.

Photocatalysis was investigated on nanostructured $SrFeO_3$ using phenol dye with 450W high pressure mercury lamp. The photocatalytic activity was greatly improved by ultrasonic radiation, with red-shifted band edge of UV-Vis adsorption spectra than that of the samples prepared by conventional method [15].

The effect of crystallite structure and the photocatalytic activity of BFO –doped nanoparticles with Ba, Na and K metal ions were investigated [16]. Novel $La_{0.5}Bi_{0.2}Ba_{0.2}Mn_{0.1}FeO_{3-\delta}$, with a perovskite-like structure, was synthesized by using the citric acid sol-gel route. The powders were all screened for photocatalytic activity against an organic dye (rhodamine B) in the visible region of the solar spectrum and the photocatalytic activities were good particularly for powders annealed at 900 °C [9].

MATERIALS AND METHODS

Reagents used were; Ammonium hydroxide, sodium dodecyl sulfate ($NaC_{12}H_{25}SO_4$), sodium nitrate ("symbolled" as M), potassium nitrate ("symbolled" as M), Strontium nitrate, $Sr(NO_3)_2$, Iron(III)nitrate-9.water, $Fe(NO_3)_3.9H_2O$, distilled water, methylene blue ($C_{16}H_{18}ClN_3S$).

Apparatus used were: Magnet, magnetic-stirrer heater, Hotbox Oven size one (England), Muffle Furnace of Nabertherm GmbH LH 120/14 (Germany), Analytical weighing balance of AC Adapter DC 12V (Japan), Spectrophotometer Sherwood 254 (UK), Solar box, Thermobalance-Perkin-Elmer (TGA 8000), Rigakuminiflex 300, pH meter of HANNA H14321 (Romania, Europe), Topcon SM-300 SEM/EDX (India).

Table 1; The Precursor Stoichiometric parameters for Synthesis of $Sr_{1-x}M_xFeO_3$

X (g)	Na_XNO_3 (g)	K_XNO_3 (g)	$Sr_{1-x}(NO_3)_2$ (g)	$Fe(NO_3)_3.9H_2O$(g)
0.0	0.0	0.0	211.62= 10.58	403.85= 20.19
0.1	8.50 = 0.43	10.11= 0.51	190.46= 9.52	403.85= 20.19
0.2	17.00 = 0.85	20.22= 1.01	169.30= 8.47	403.85 =20.19

An addition of calculated stoichiometric amount of strontium nitrate, Iron (III) nitrate-9.water, sodium nitrate in their proportions was dissolved in distilled water as required and stirred well before heating . Then a magnet was introduced into the solution and heated on magnetic-

stirrer for 20-25 minutes at 90 °C that ensured thorough mixing of metals. After which 50% sulfactant, SDS, was added and 5mins later precipitated with NH_4OH in drops, filtered, washed twice with 100 ml of distilled water and oven-dried for 14hrs at 80 ^oC [17].

The process was repeated using potassium doped material for the synthesis in its calculated stoichiometric amounts. The synthesised-doped perovskites, were then annealed at 500 ^oC, 700 ^oC and 800 ^oC for 2 hrs in muffle furnace, each of sodium and potassium doped samples [18].

Characterization of Undoped and Na/ K-Doped Perovskites

X-Ray Diffractometry

The PXRD was done using Rigakuminiflex 300 (Cu-Kα) with a step size of 10^{o}C/min scan rate from 0-80^{o}2θ values. The PXRD machine, has sample introduced containing finely grounded crystallite size determination using Scherrer's equation, sample purity and residual strain of the powders.

Scherrer's equation: $D = \frac{k\lambda}{\beta\cos\theta}$

Where D is crystallite size, k is machine constant (0.9), λ is wavelenght of CuKα (1.5406A^o), β is the full width of half maximum and θ is half of 2θ.

Scanning Electron Microscopy

The SEM, (Topcon SM-300 LEO 1530) for morphology showing topographical observation of micrographs on the synthesized powder was carried out. Powdered sample was mounted on sputtered white epoxy resin and put in the SEM machine. The energy dispersive spectroscopy was conducted with electron probe microanalyzer(for the qualitative) to show the weight concentration of sample constituents and qualitative analysis by graphical representation of sample elemental analysis.

Photocatalysis Test

The Methylene-Blue (volume = 5.0 ml, concentration = 1.0 x 10^{-5} M) was mixed with the sample using a magnetic stirrer at 50 rpm and degradation experiments were performed under simulated solar light by means of a Solarbox (improvised) 3000e RH testing instrument equipped with a Xe lamp (250 W). The UV–Vis irradiance time was varied at a uniform interval by a Delta Ohm HD 232.0 photo-radiometer. The MB concentration was determined by UV-Vis Spectrophotometer for every sample at interval of 20 mins for 2 hrs. The photocatalytic activity

was then evaluated by monitoring the dye absorbance maximum at λ_{max} = 664 nm of the dye operating at an approximate pH 6.8. The MB degradation efficiency was calculated as:

$$D.E = (1 - C/C_o) \times 100\ (\%),$$

Where D.E is degradation efficiency, C and C_o are the concentration values for the sample and the control solution, respectively (estimated uncertainty = ±4%) in order to determine the concurrence of main factor, that is the light harvesting capability.

RESULTS AND DISCUSSION

Table 2: Some PXRD parameters of Na-doped synthesized material at 800 ºC

No.	2-theta(deg)	d(ang.)	Height(counts)	FWHM(deg)	Asym. Factor
1	27.4639	3.245	105.11	0.349	1.0663
2	28.4845	3.131	72.04	0.3405	1.0513
3	30.4734	2.93104	101.19	0.3926	1.0751
4	33.3974	2.6808	58.14	1.0117	0.737
5	44.6585	2.02748	84.66	0.4086	0.8541
6	45.6302	1.98654	74.52	0.3942	1.0199

Table 3: Some PXRD parameters of K-doped synthesized material at 800 ºC

No.	2-theta(deg)	d(ang.)	Height(counts)	FWHM(deg)	Asym. factor
1	24.595	3.61663	16.21	2.0987	4.5653
2	26.2407	3.39342	43.49	0.2911	0.699
3	27.4438	3.24732	144.27	0.3517	1.3074
4	28.4064	3.13943	82.55	0.3803	0.8089
5	30.4396	2.93421	158.49	0.3363	1.011
6	33.0905	2.70495	103.53	0.3783	0.6176

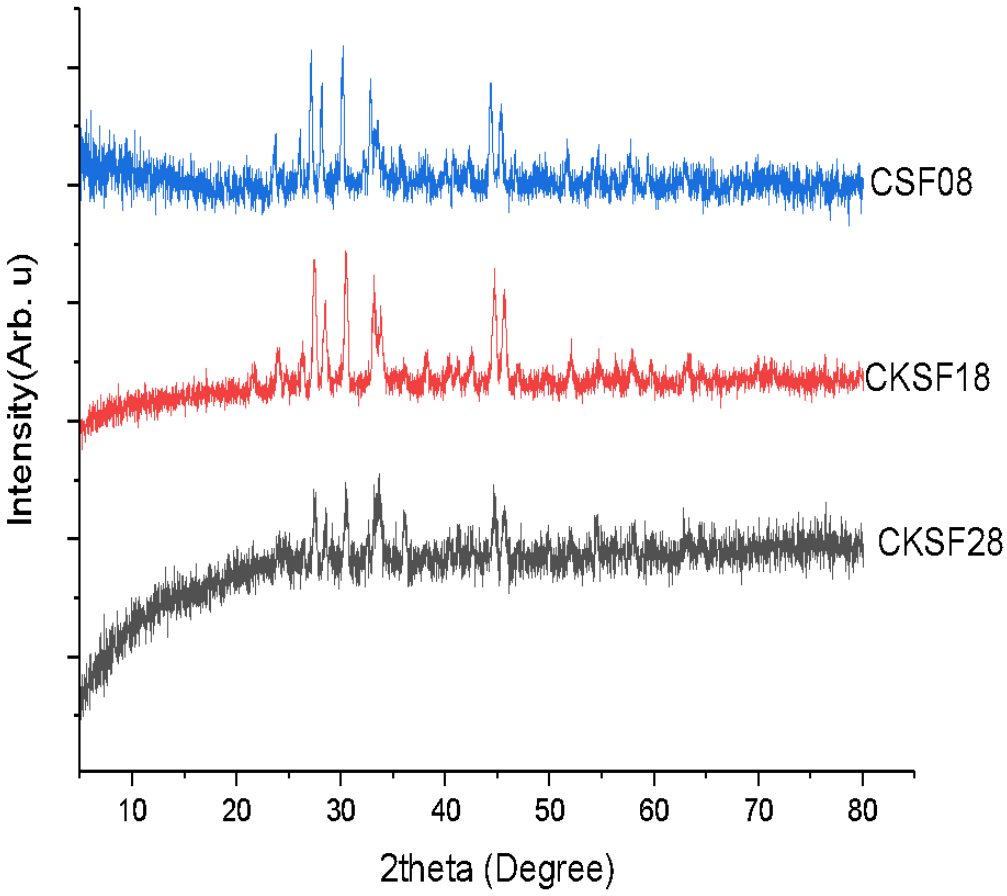

Figure 1: PXRD Result Depicting undoped (x=0) and K-doped, $Sr_{1-x}K_xFeO_3$, (x=0.1 and 0.2) Perovskites Annealed at 800 ºC.

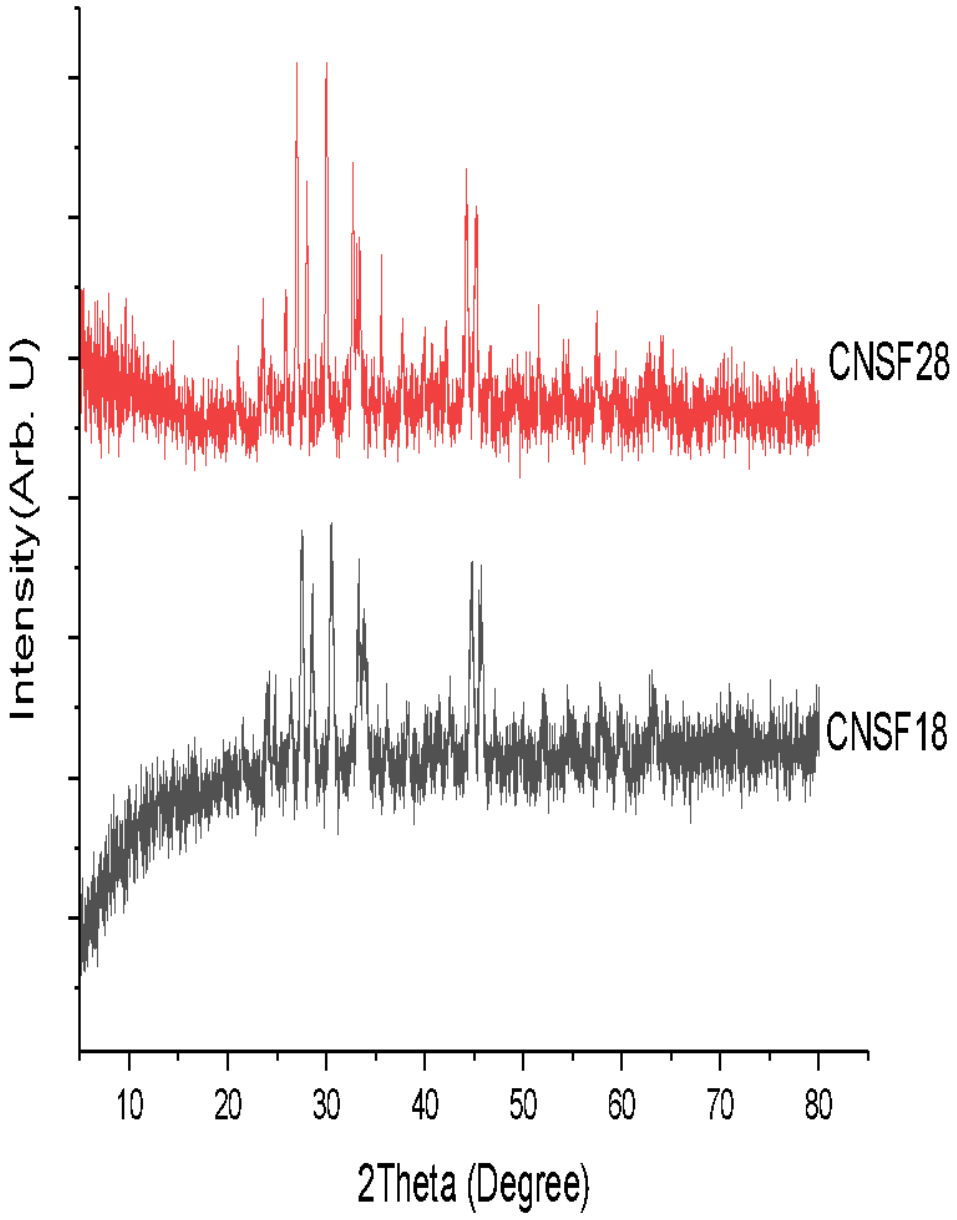

Figure 2: PXRD Result Depicting Na-doped (x=0.1 and 0.2) Perovskites ($Sr_{1-x}Na_xFeO_3$) Annealed at 800 ^oC

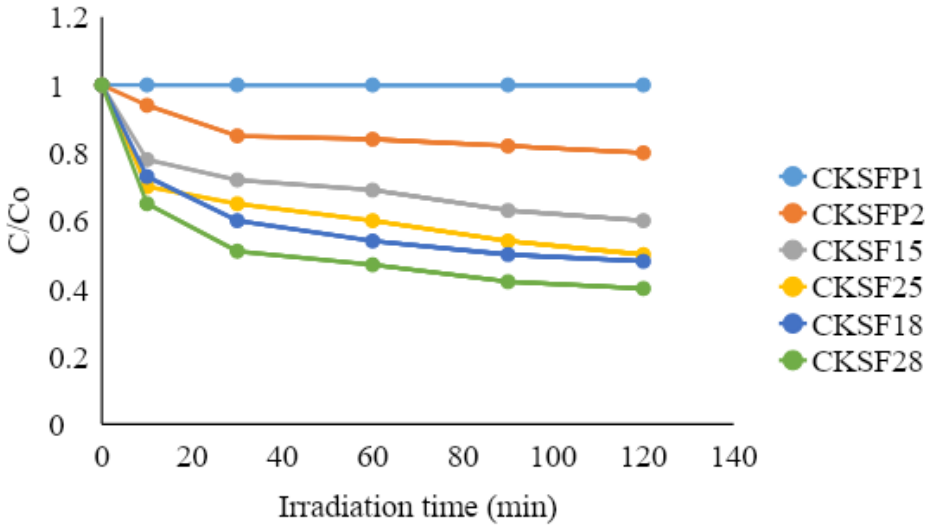

Figure 3: MB Photocatalytic Degradation Promoted by $Sr_{1-x}M_xFeO_3$ (x=0.1 and 0.2) K-doped Perovskite of Raw and Annealed at 500 ºC and 800 ºC activated by Simulated solarlight

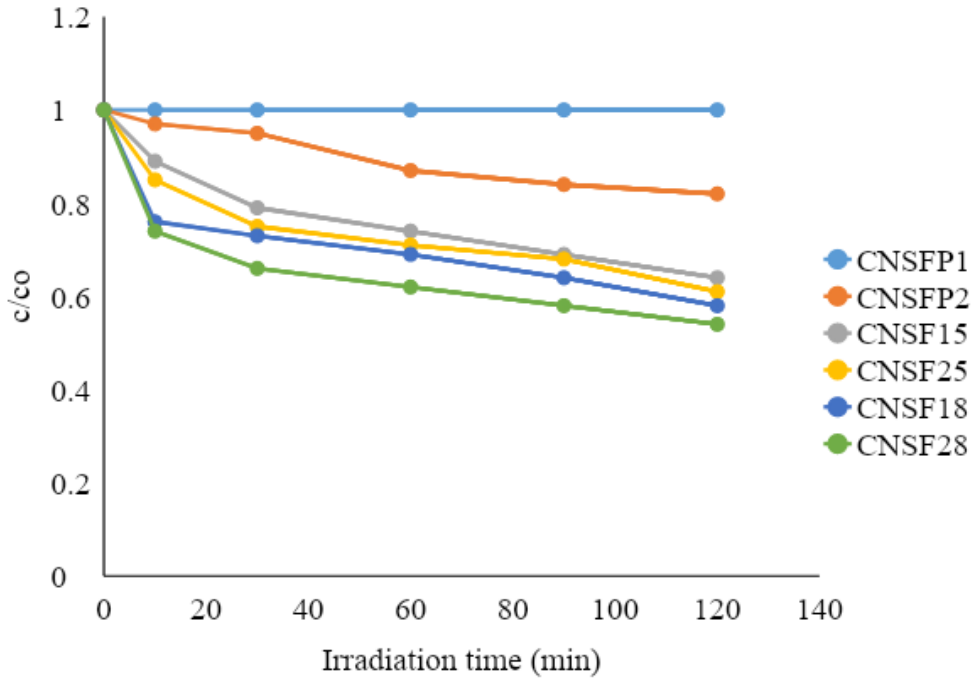

Figure 4: MB Photocatalytic Degradation Promoted by $Sr_{1-x}M_xFeO_3$(x=0.1 and 0.2) Na-doped Perovskite of Raw and Annealed at 500ºC and 800ºC activated by Simulated solarlight

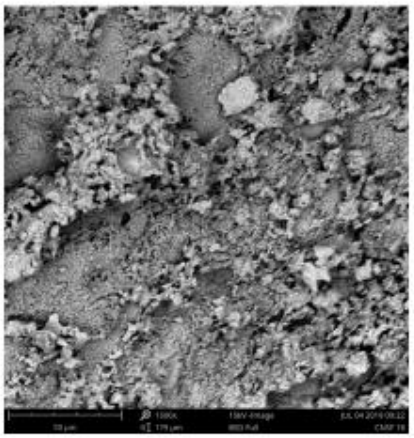

Figure4.8; SEM Result of Na-doped Synthsized Sample, $Na_{0.1}Sr_{0.9}Fe_2O_3$, annealed at 800oC

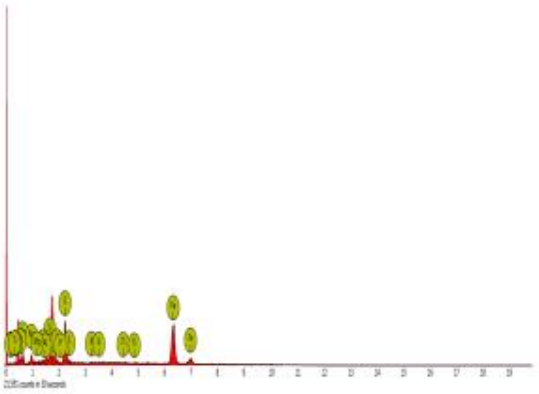

EDS of Na-doped, $Na_{0.1}Sr_{0.9}Fe_2O_3$ at 800°C

Plate 1: SEM and EDS of Na-doped with X = 0.10g annealed at 800°C

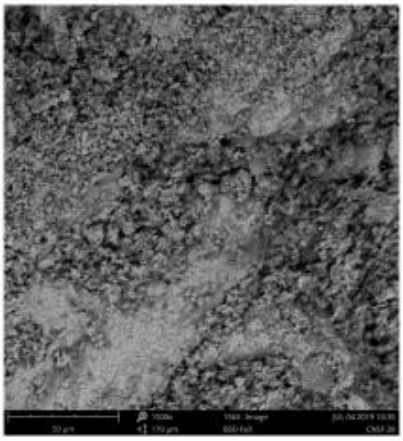

Figure 4.9; SEM Result of Na-doped Synthsized Sample, $Na_{0.2}Sr_{0.8}Fe_2O_3$, annealed at 800°C

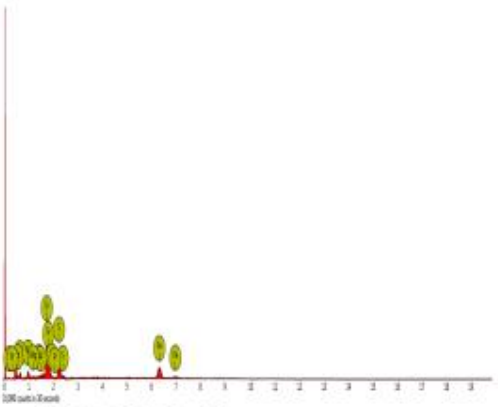

EDS of Na-doped, $Na_{0.2}Sr_{0.8}Fe_2O_3$

Plate 2: SEM and EDS of Na-doped with X = 0.20g annealed at 800°C

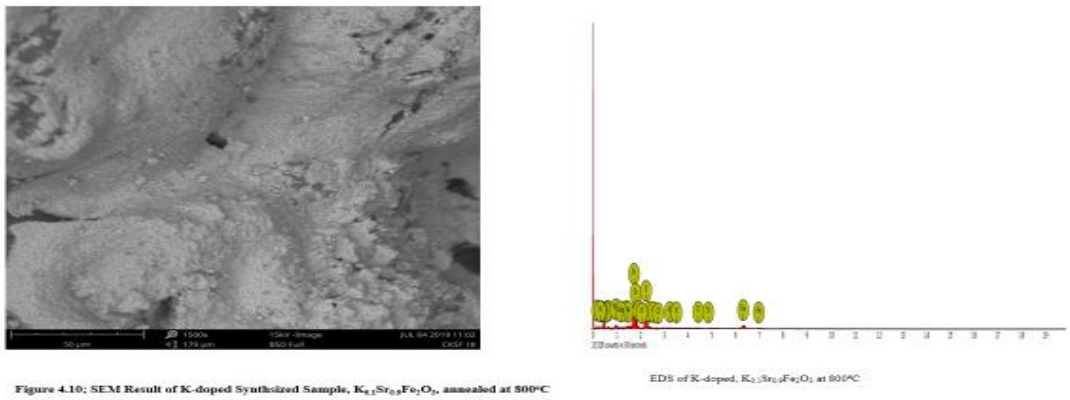

Figure 4.10; SEM Result of K-doped Synthsized Sample, $K_{0.1}Sr_{0.9}Fe_2O_3$, annealed at 800°C

EDS of K-doped, $K_{0.1}Sr_{0.9}Fe_2O_3$ at 800°C

Plate 3: SEM and EDS of K-doped with X = 0.20M annealed at 800°C

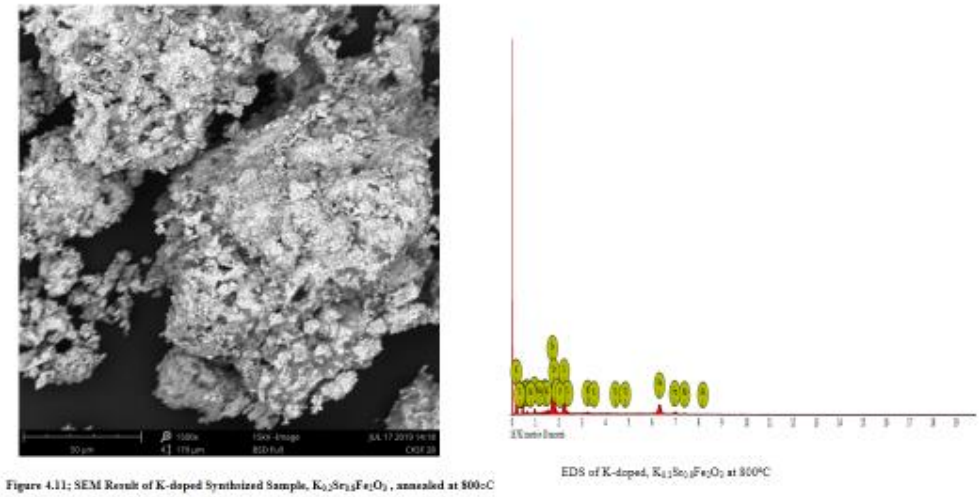

Figure 4.11; SEM Result of K-doped Synthsized Sample, $K_{0.2}Sr_{0.8}Fe_2O_3$, annealed at 800oC

EDS of K-doped, $K_{0.1}Sr_{0.9}Fe_2O_3$ at 800°C

Plate 4: SEM and EDS of K-doped with X = 0.10M annealed at 800°C

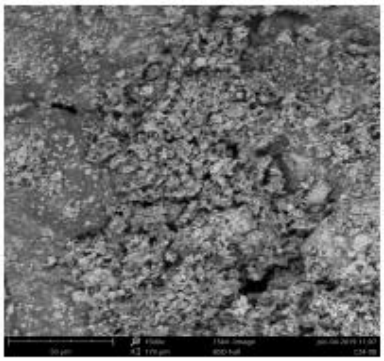

Figure4.7; SEM Result of undoped Synthsized Sample, $SrFe_2O_3$, annealed at 800°C

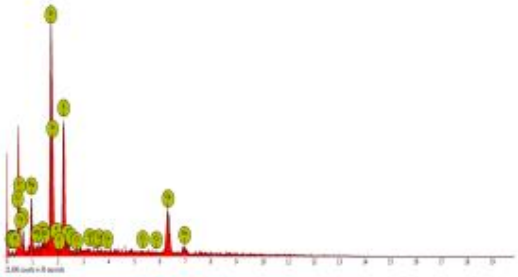

EDS of undoped, CSF08, $SrFe_2O_3$ at 800°C

Plate 5: SEM and EDS of undoped with X = 0.00M annealed at 800°C

Scan Electron Microscopy

The 50µm at magnification of 1500x backscattered image detector (BSD) full of all the samples surface hexagonal morphology in plate 1-5 by secondary electron image (SEI) were obtained with Nadopant depicting a nonconspicuous grey pattern due to its low concentration and less reactive nature unlike $K_{0.1}NO_3$. For every SEM obtained EDS was examined for compositional observation and inferred a qualitative analysis of elements contained in the synthesized samples with much purity considering the weight concentration of their constituents.

Photocatalytic Analysis

The raw control sample, Na-doped at x=0.1, was not exposed to solar light after its mixture with the MB and has a 100% degradation efficiency regardless of its irradiation time. The K-doped sample at x=0.2 annealed at 800 °C has the most efficient degradation pattern as temperature increased, due to its reactiveness and higher concentration used. Very close degradation was observed between the K-doped at x=0.2 for 500 °C and Na-doped at x=0.1 for 800 °C.

Powdered X-Ray Diffractometry

PXRD of the perovskite peak at 27° 2θ shown in fig 1-2. The sample crystallized, $Sr_{1-x}M_xFeO_3$, hexagonal structure was distorted and formed orthorhombic by the addition of $Na^+$and K^+ has the PXRD showed more prominent peaks of Sr and Fe at their assigned positions in all the samples. With a very fine-powdered samples used, the peaks have some resemblance where the particle size of K-doped was 0.258nm, 0.303nm for Na-doped and 0.239nm for the undopedperovskite. The peak formed depended on precipitation temperature of the precursor and their temperature in the muffle furnace.

CONCLUSION

The EDS qualitative and quantitative measurement had revealed the actual SEM micrograghical topography of the sample. The use of MB in the photocatalysis of $Sr_{1-x}M_xFeO_3$ confirmed that K-doped sample for x=0.2 at 800°C has most efficient degradation for all irradiation time engaged. The PXRD results were true analysis ofcationically doped perovskite with all peaks aligned on same position in the 2θ axis between 25-50°. It was clear that for coprecipitation method the crystallization temperature of $Sr_{1-x}M_xFeO_3$ depended upon the precipitation temperature of the precursor and that of the MuffleFurnace. With increasing the values of x, the concentration of unstable Fe^{3+} and/or of oxygen vacancies also in- crease, which favors the diffusion of lattice oxygen from the bulk to surface, as charge compensators. Thus, increasing the "M" content in the defective structure of $Sr_{1-x}M_xFeO_3$ accounts for the unstability of the lattice in a reducing environment.

REFERENCES

1. Lowell, M., Norimasa, N., Yanbin, W., Atsushi, K., Don, V.W., Robert, J.C., Thomas, S.D. & Wenk, H. (2008). Deformation and texture development in $CaIrO_3$ post-perovskite phase up to 6 GPa and 1300 K, *Earth and Planetary Science Letters*, 268 (3–4): 515-525, https://doi.org/10.1016/j.epsl.2008.02.005.
2. Bennett, V.C. (2003). Compositional Evolution of the Mantle, *Treatise on Geochemistry*, 2, 493-519, https://doi.org/10.1016/B0-08-043751-6/02013-2
3. Salamon, M.B. & Jaime, M. (2001). EstudioMediante XPS de Un Acero al CarbonoImplantado Con NitrogenoporMedio de Descargas de Alto Voltaje a BajasPresiones. *Rev. Mod. Phys*. 73, 583.

4. Loktev, V.M. & Pogorelov, Yu.G. (2000). Peculiar Physical Properties and the ColossialMagnetoresistance of Manganites, *Low Temp. Phys*. 26, 231- 261. DOI: 10.1063/1.593890
5. Akao, T., Azuma, Y., Usuda, M., Nishihata, Y., Mizuki, J., Hamada, N., Hayashi, N., Terashima, T. & Takano, M. (2003). Charge-ordered state in single-crystalline $CaFeO_3$ thin film studied by X-ray anomalous diffraction, *Phys. Rev. Lett*. 91, 156405.
6. Ying, Wu. & Du-Lin, Y. (2003). Hydroxonium 1-ammonioethylidene-1,1-bisphosphonate, *Prog. Solid State Chem*. 31(4), 239.
7. Ketov, S.V., Yagodkin, Yu.D. & Menushenkov, V.P. (2010). Structure and magnetic properties of strontium ferrite anisotropic powder with nanocrystalline structure, *J. of Alloys and Compounds*. 2(5), 1066.
8. Mitzi, D.M. (2001b). Thin-film deposition of organic-inorganic hybrid materials. *Chem. Mater*., 13(10), 3283–3298.
9. Abdulkadir, I., Jonnalagadda, S.B., Martincigh, B.S. (2016). Synthesis and effect of annealing temperature on the structural, magnetic and photocatalytic properties of $(La_{0.5}Bi_{0.2}Ba_{0.2}Mn_{0.1})FeO_{(3-d)}$. *Mater. Chem. Phys*. 178, 196–203. https://doi.org/10.1016/j.matchemphys.2016.05.007.
10. Kodama, R.H., Makhlouf, S.A. & Berkowitz, A.E. (1997). Finite Size Effects in Antiferromagnetic NiO Nanoparticles, *Phys. Rev. Lett*. 79,1393.
11. Suresh, K., Panchapagesan, T.S. & Patil, K.C. (1999). Synthesis and Properties of $La_{1-x}Sr_xFeO_3$, *Solid State Ionics* 126 (3-4): 299-305.
12. Mukherjee, S., & Chakraborty, S. (2012). Evidence for the Direct Decay of the 125 GeV Higgs boson to Fermions, *Int. J. Current Engineeringand Technology* **12,** 403.
12. Zhang, Z., Liu, H. & Xuliang, D. (2012). Influence of La doping on Magnetic and Optical Properties of bismuth Ferrite Nanofibers, *J. of nanometer*. DOI: 10.1155/2012/238605
12. Praveen, A. Duhan, S. & Pratima, S. (2008). Effect of thermal annealing on Nd_2O_3-doped silica powder prepared by the sol-Gel process, *J. SolGel Sci. and Tech.* DOI:10.1007/s10971-008-1691-6.
13. Jia, L., Ding, T., Li, Q. & Tang, Y. (2007). Study of Photocatalytic performance of $SrFeO_{3-x}$ by Ultrasonic radiation, *Catalysis Communication,* 8 (6): 963-966.

16. Haruna, A., Abdulkadir, I. & Idris, S.O. (2019). Synthesis, characterization and photocatalytic properties of $Bi_{0.85-x}M_xBa_{0.15}FeO_3$ (M = Na and K, X = 0, 0.1) perovskite-like nanoparticles using the sol-gel method. *Journal of King Saudi University – Science* https://doi.org/10.1016/j.jksus.2019.05.005
17. Jianlan, T., Mankang, Z., Tao, Z., Yudong, H.W. & Hui, Y. (2007). Synthesis of Fine $Pb(Fe_{0.5}Nb_{0.5})O_3$Perovskite Powders by coprecipitation Method, *Mat. Chem. and Phys*. 101, 475-479.
18. Hye, J.Y., Singha, S.M. & Jae, W.C. (2014). High-Speed Actuation and Mechanical Properties of Graphene-Incorporated Shape Memory Polyurethane Nanofibers, *Journal of Physical Chemistry* CSCI(E)4, 31